AGU PUBLICATIONS

JGR

Journal of Geophysical Research: Biogeosciences

RESEARCH ARTICLE

10.1002/2016JG003671

**Key Points:**
- Arctic tundra ecosystem is an annual net source of $CO_2$
- Winter $CO_2$ release offsets growing season $CO_2$ gain
- Active layer thickness is a significant driver of NEE, GPP, and $R_{eco}$

**Supporting Information:**
- Supporting Information S1

**Correspondence to:**
G. Celis,
gerardo.celis@nau.edu

**Citation:**
Celis, G., M. Mauritz, R. Bracho, V. G. Salmon, E. E. Webb, J. Hutchings, S. M. Natali, C. Schädel, K. G. Crummer, and E. A. G. Schuur (2017), Tundra is a consistent source of $CO_2$ at a site with progressive permafrost thaw during 6 years of chamber and eddy covariance measurements, *J. Geophys. Res. Biogeosci.*, *122*, 1471–1485, doi:10.1002/2016JG003671.

Received 16 OCT 2016
Accepted 21 MAY 2017
Accepted article online 30 MAY 2017
Published online 28 JUN 2017



# Tundra is a consistent source of $CO_2$ at a site with progressive permafrost thaw during 6 years of chamber and eddy covariance measurements

**Gerardo Celis[1,2], Marguerite Mauritz[1], Rosvel Bracho[3], Verity G. Salmon[4], Elizabeth E. Webb[2], Jack Hutchings[2], Susan M. Natali[5], Christina Schädel[1], Kathryn G. Crummer[6], and Edward A. G. Schuur[1,2]**

[1]Center for Ecosystem Science and Society, Northern Arizona University, Flagstaff, Arizona, USA, [2]Biology Department, Bartram Hall, University of Florida, Gainesville, Florida, USA, [3]School of Forest Resources and Conservation, University of Florida, Gainesville, Florida, USA, [4]Environmental Sciences Division, Climate Change Science Institute, Oak Ridge National Laboratory, Oak Ridge, Tennessee, USA, [5]Woods Hole Research Center, Falmouth, Massachusetts, USA, [6]Institute for Sustainable Food Systems, University of Florida, Gainesville, Florida, USA

**Abstract** Current and future warming of high-latitude ecosystems will play an important role in climate change through feedbacks to the global carbon cycle. This study compares 6 years of $CO_2$ flux measurements in moist acidic tundra using autochambers and eddy covariance (Tower) approaches. We found that the tundra was an annual source of $CO_2$ to the atmosphere as indicated by net ecosystem exchange using both methods with a combined mean of 105 ± 17 g $CO_2$ C $m^{-2}$ $y^{-1}$ across methods and years (Tower 87 ± 17 and Autochamber 123 ± 14). The difference between methods was largest early in the observation period, with Autochambers indicated a greater $CO_2$ source to the atmosphere. This discrepancy diminished through time, and in the final year the Autochambers measured a greater sink strength than tower. Active layer thickness was a significant driver of net ecosystem carbon exchange, gross ecosystem primary productivity, and $R_{eco}$ and could account for differences between Autochamber and Tower. The stronger source initially attributed lower summer season gross primary production (GPP) during the first 3 years, coupled with lower ecosystem respiration ($R_{eco}$) during the first year. The combined suppression of GPP and $R_{eco}$ in the first year of Autochamber measurements could be the result of the experimental setup. Root damage associated with Autochamber soil collar installation may have lowered the plant community's capacity to fix C, but recovered within 3 years. While this ecosystem was a consistent $CO_2$ sink during the summer, $CO_2$ emissions during the nonsummer months offset summer $CO_2$ uptake each year.

## 1. Introduction

High-latitude ecosystems are among the global ecosystems that will experience greatest increases in air temperature by the end of the century due to climate amplification [*International Panel on Climate Change (IPCC)*, 2014]. These ecosystems store large stocks of carbon (C) in soils, in particular in perennially frozen soils (permafrost), which currently contain approximately 1330–1580 PgC in the form of frozen soil organic matter [*Tarnocai et al.*, 2009; *Hugelius et al.*, 2014; *Schuur et al.*, 2015]. Current warming in high-latitude regions is associated with soil warming and permafrost thaw [*Romanovsky et al.*, 2011; *IPCC*, 2014], which has the potential to release large amounts of stored C to the atmosphere. An estimated 130 to 160 PgC will be released by 2100 under a high warming scenario (i.e., Representative Concentration Pathway scenario 8.5) [*Schuur et al.*, 2015], and these C emissions are expected to accelerate the rate of global climate change [*Koven et al.*, 2011].

The net contribution of $CO_2$ from high latitudes to the atmosphere will depend on the balance between two major processes: (a) decomposition and/or physical release of soil C reserves [*Xue et al.*, 2016] and (b) the capacity of vegetation to fix atmospheric $CO_2$ during the growing season [*Schimel*, 1995; *Lucht et al.*, 2002; *Walker et al.*, 2012]. The drivers that will influence $CO_2$ fluxes can be physical and/or biological [*McGuire et al.*, 2009]. Physical drivers that have the potential to alter $CO_2$ fluxes are longer snow-free periods [*Groendahl et al.*, 2007; *Euskirchen et al.*, 2009; *Lund et al.*, 2012], increased temperature [*Rustad et al.*, 2000; *Davidson and Janssens*, 2006], reduced soil moisture [*Oberbauer et al.*, 2007; *Sharp et al.*, 2013; *Natali et al.*, 2015], and increased nutrient availability [*DeMarco et al.*, 2014; *Salmon et al.*, 2016]. Biological drivers potentially tied to fluxes are improved species performance [*Chapin and Shaver*, 1985; *Oberbauer et al.*, 2013], shift in plant communities [*Walker et al.*, 2006; *Schuur et al.*, 2007; *Myers-Smith et al.*, 2011; *Hollister et al.*, 2015], and herbivory [*Welker et al.*, 2004; *Kelsey et al.*, 2016]. The warming of soils and thawing of permafrost stimulate soil organic matter decomposition [*Mackelprang et al.*, 2011; *Schädel et al.*, 2014; *Xue et al.*, 2016] and increase heterotrophic respiration from soils result in a positive feedback to the atmospheric $CO_2$ concentration but will depend on snow accumulation [*Nowinski et al.*, 2010; *Blanc-Betes et al.*, 2016] and changes in soil community abundance and composition [*Mohan et al.*, 2014; *Morgado et al.*, 2015; *Parker et al.*, 2015; *Semenova et al.*, 2015; *Geml et al.*, 2016; *Morgado et al.*, 2016]. Increased $CO_2$ loss may, however, be counteracted by increases in net primary production (NPP) as plant productivity increases [*Epstein et al.*, 2012] and the plant community shifts from graminoid to shrub dominance [*Sturm et al.*, 2005; *Walker et al.*, 2006; *Myers-Smith et al.*, 2011; *Pearson et al.*, 2013; *Hollister et al.*, 2015]. There is considerable variability among observational studies and modeling approaches [*Koven et al.*, 2011], with some reviews showing annual $CO_2$ emissions exceed $CO_2$ uptake [*Belshe et al.*, 2013], while others indicate that the tundra is a net $CO_2$ sink [*McGuire et al.*, 2012, and references therein]. There is growing evidence that winter is an important driver of annual estimates since cold season losses which can offset summer season gains [*Fahnestock et al.*, 1999; *Welker et al.*, 2000; *Euskirchen et al.*, 2012; *Grogan*, 2012; *Oechel et al.*, 2014]. Yet winter remains one of the most uncertain periods of the Arctic $CO_2$ balance. In the past it has been difficult to constrain Arctic $CO_2$ fluxes due to spatially and temporally sparse measurements, and differences in measurement techniques. Better estimates of both the magnitude and direction of $CO_2$ fluxes (i.e., net source or sink) is critical for understanding the strength of the Arctic carbon-climate feedback.

Studies related to $CO_2$ fluxes measurements are often collected at different spatial scales. Small-scale ($<1$ m$^2$) measurements are used to understand the dynamics of manipulative experiments (e.g., the International Tundra Experiment, ITEX [*Henry and Molau*, 1997]) and local processes that affect $CO_2$ cycling. Small-scale measurements provide important mechanistic insights for $CO_2$ fluxes but can be difficult to scale and be biased by site selection [*Fox et al.*, 2008]. Eddy covariance towers are used at larger scales ($>$10,000 m$^2$) to observe landscape dynamics and can incorporate a wide range of microsite conditions and vegetation types, which affect the $CO_2$ balance [*Belshe et al.*, 2012] but may not capture mechanistic processes. The process of data comparison for landscape-level analysis is further complicated by the fact that many studies only utilize one method to measure $CO_2$ fluxes at a given site. It is well documented that measured $CO_2$ flux estimates vary depending on the method employed [*Björkman et al.*, 2010; *Riederer et al.*, 2014; *Webb et al.*, 2016] and colocated measurements of $CO_2$ fluxes using different methods can differ due to the small scale changes in the local plant community, time of day, and time of year [*Oechel et al.*, 1998; *Smith et al.*, 2003; *Myklebust et al.*, 2008]. Accurate quantification of the Arctic $CO_2$ balance relies on the ability to combine and compare chamber and tower based data, but there is a scarcity of research on how these two methods differ from one another. The present study provides an opportunity to compare these two measurement techniques and determine both the magnitude and direction of $CO_2$ fluxes (i.e., net source or sink) in a rapidly thawing tundra ecosystem.

This study examined the dynamics of ecosystem $CO_2$ exchange using two complementary methods of measuring $CO_2$ fluxes: (a) plot-scale experiment ($<1$ m$^2$ scale using autochambers) and (b) landscape observation ($>$10,000 m$^2$ using eddy covariance) measurements. We addressed the following questions: (1) Is tundra a net annual $CO_2$ source or sink at a site with permafrost thaw? (2) What are seasonal and interannual changes in $CO_2$ magnitude, and what environmental variables drive these changes? (3) Do measurements at different scales (eddy covariance tower and autochambers) show the same magnitude and variability?

## 2. Methods

### 2.1. Site Descriptions and Setup

Carbon dioxide flux measurements were measured within a discontinuous permafrost zone at the Eight Mile Lake (EML) research site near Healy, Alaska, USA [*Schuur et al.*, 2007, 2009; *Vogel et al.*, 2009; *Lee et al.*, 2010, 2011; *Natali et al.*, 2011; *Belshe et al.*, 2012; *Natali et al.*, 2012; *Trucco et al.*, 2012; *Hicks Pries et al.*, 2013a, 2013b; *Natali et al.*, 2014, 2015; *Salmon et al.*, 2016; *Webb et al.*, 2016; *Mauritz et al.*, 2017]. The site contains a permafrost borehole which has documented rising permafrost temperatures since 1985 [*Osterkamp and Romanovsky*, 1999], and within the past three decades the site has experienced varying levels of disturbance associated with permafrost thaw [*Schuur et al.*, 2007]. The site vegetation community depends on permafrost degradation. Low and intermediate thaw stages are dominated by the graminoid *Eriophorum vaginatum*, a tussock-forming sedge, whereas in the transition to extensively thawed permafrost shrubs (evergreen—*Rhododendron subarcticum* and deciduous—*Vaccinium uliginosum*) become dominant [*Schuur et al.*, 2007]. Landscape-scale $CO_2$ fluxes have been monitored since June 2008 using the eddy covariance approach (hereafter called Tower; 63°52′42″N, 149°13′12″W). Small-scale $CO_2$ fluxes were measured at the plot level (0.36 $m^2$) from the Carbon in Permafrost Experimental Heating Research project (hereafter called Autochamber; 63°52′59″N, 149°13′32″W), which was initiated in September 2008 and was designed to simulate anticipated increases in soil and air temperatures [*Natali et al.*, 2011]. Because the goal of this analysis was to evaluate how permafrost thaw impacts $CO_2$ fluxes under ambient climate forcing, only control plots, which did not receive any warming treatment, were used in this analysis. Control plots were selected from within the blocked split-plot warming experiment which used snow fences and open top chambers (OTCs, 50 cm tall constructed of 0.6 cm thick clear polycarbonate) to simulate warming; there were two control plots (60 × 60 cm) at each of the six snow fences, so we used a total of 12 replicate plots for this study. Further description of the field site and warming experiment can be found in [*Natali et al.*, 2011, 2012]. Autochamber plots are located just outside the tower fetch, and soil classification, climatic conditions, topography, and vegetation community were similar between Autochamber and Tower [*Schuur et al.*, 2007; *Natali et al.*, 2011, 2012]. A high-resolution active layer thickness (ALT) survey ($n$ = 310) in 2008 and 2009 at the Tower showed that ALT ranges at Tower and Autochamber plots encompassed similar ranges throughout the study period [*Belshe et al.*, 2012]. The Tower included few areas with more extensive permafrost thaw than was documented at Autochamber. Based on 2009 plot-level census (Tower $n$ = 225 and Autochamber $n$ = 12), vegetation is dominated by moist acidic tussock tundra comprising an average mixture of ~11–29% sedges (*Eriophorum vaginatum*), ~23–25% deciduous and ~25–29% evergreen shrubs (*Vaccinium uliginosum*, *Rubus chamaemorus*, *Betula nana*, and *Rhododendron subarcticum*), and ~20–39% nonvascular plants (*Sphagnum* spp., *Dicranum* spp., feathermoss, and lichens) [*Salmon et al.*, 2016].

### 2.2. Environmental Monitoring

An Onset HOBO (Bourne, MA) weather station measured environmental parameters including air temperature, rainfall, and photosynthetically active radiation (PAR) at Autochamber. The Tower data were collected at an adjacent station, which included PAR (Li-190SA, LI-COR Biosciences), incident radiation (Li-200SA, LI-COR Biosciences), net radiation (REBS Q*7.1, REBS Inc., Seattle, Washington), relative humidity and air temperature (Vaisala HMP45c, Campbell Scientific), and wind speed and direction (RM Young 3001, Campbell Scientific). Soil temperatures (10 cm depth) were measured continuously in each plot at Autochamber and in two locations at Tower using constantan-copper thermocouples. Active layer thickness (ALT; end of summer season maximum thickness of thawed ground) was measured in each plot at Autochamber and at nine locations within the Tower footprint using a metal depth probe. Water table depth (WTD) was measured from 12 water wells at Autochamber and 9 wells at Tower. Thaw and water table depth measurements were colocated with reported observations of the plant community, and so these measurements capture the range of environmental conditions experienced by the plant communities at this site, and the range of microsites integrated by the tower.

### 2.3. Carbon Flux Measurements

Net ecosystem carbon exchange (NEE) was measured using two different approaches: (1) landscape dynamics using an eddy covariance tower and (2) localized plot measurements using autochambers. During the summer season both methods were simultaneously deployed; during the nonsummer season $CO_2$ fluxes were estimated by a combination of manual chamber flux measurement and models parameterized with Tower measurements and method-specific soil temperatures. Negative NEE indicate $CO_2$ uptake by the ecosystem.

Autochamber NEE (μmol $CO_2$ C $m^{-2}$ $s^{-1}$) and ecosystem respiration ($R_{eco}$ μmol $CO_2$ C $m^{-2}$ $s^{-1}$) were measured using automated $CO_2$ flux systems during the summer (May–September) of 2009–2014. Automated flux chamber (0.36 $m^2$ × 0.25 m) measurements were made continuously (every 1.5 h) at 12 plot locations and averaged per fence ($n$ = 6). Automated chamber measurements were supplemented with weekly manual chamber measurements from October to November, in order to capture fall-season dynamics and before snow cover impeded further measurements. For both automated and manual measurements air was circulated within the chamber and $CO_2$ concentrations were sampled in 2 s intervals at 1 L $min^{-1}$, for 1.5 min, using an infrared gas analyzer (LI-820, LICOR Corp., Lincoln, Nebraska), and recorded on a data logger (Campbell Scientific CR1000 in the summer and Arduino unit in the fall). NEE flux rates were calculated using linear regression and converted from volumetric (ppm $CO_2$ $m^2$ $s^{-1}$) to mass (μmol $CO_2$ $m^{-2}$ $s^{-1}$) using plot-specific chamber volumes and air temperatures. Flux data were quality controlled for outlying and erratic fluxes based on equipment failure and environmental conditions known to produce erratic fluxes (i.e., wind speeds exceeding 7 m $s^{-1}$). After screening, at least 80% of total flux measurements were retained. A more detailed description of the setup and data processing can be found in [*Natali et al.*, 2011, 2014; *Mauritz et al.*, 2017].

Tower NEE was measured using eddy covariance (EC) starting May 2008 to September 2014.The system consisted of a sonic anemometer (CSAT3, Campbell Scientific, Logan, Utah), and an open path infrared gas analyzer (Li-7500, LI-COR Biosciences, Lincoln, Nebraska) mounted on a 2 m tower from 2008 to May 2011 after which sensors were raised to 3.5 m and a Li-7500A $CO_2$ analyzer was installed. High-frequency data for $CO_2$, water vapor, orthogonal wind components (*u*, *v*, and *w*), and air temperature were recorded at 10 Hz using a CR500 data logger (Campbell Scientific). Calibration was performed at least twice a year using a zero $CO_2$ air source, an atmospheric $CO_2$ standard (±1%), and a dew point generator (Li-610, LI-COR Biosciences) for water vapor. The internal sensor head temperature for Li-7500A was changed when mean ambient temperature reached 5°C. Fluxes were estimated from 30 min averaged covariance of $CO_2$ and vertical wind speed using EdiRe software (University of Edinburgh). Fluxes were corrected for frequency loss, sensor separation, and misalignment of wind sensors with respect to the local streamline [*Foken and Wichura*, 1996; *Aubinet et al.*, 2000], and air density [*Webb et al.*, 1980; *Burba et al.*, 2008]. Postprocessing screening eliminated data when (1) half-hour data was incomplete, (2) frictional speed ($U^*$) was $<0.12$ m $s^{-1}$ [*Goulden et al.*, 1996], and (3) variation of the half-hourly orthogonal wind components exceeded one standard deviation distance from the mean. Further detailed description (quality control and filtering) is available in *Belshe et al.* [2012] and percentages of measured data can be found in Table S1 in the supporting information. The Tower footprint from the tower estimate ranged from 200 m to 350 m [*Kormann and Meixner*, 2001] and covered a similar vegetation and permafrost thaw gradient at both height footprints. The influence of these more extensive permafrost thaw areas on Tower $CO_2$ fluxes was analyzed with a spatially explicit model that accounts for microtopography caused by permafrost degradation and it was compared to a nonlinear model presented in this manuscript that did not substantially differ in aggregated $CO_2$ predictions throughout 2008 and 2009 [*Belshe et al.*, 2012].

### 2.4. Gap Filling and Budget Calculations

Fluxes were divided into nonsummer season (1 October through 30 April the following year) and the following summer season (1 May to 30 September) and gap filled using season-specific models.

#### 2.4.1. Summer Gap Filling

Gaps in summertime NEE due to filtering and missing values were filled using a weekly hyperbolic light-response equation during high light conditions [*Thornley and Johnson*, 1990] (Text S1 and equation (S1); PAR ≥ 10 μmol $m^{-2}$ $s^{-1}$ Tower and PAR ≥ 5 μmol $m^{-2}$ $s^{-1}$ Autochamber). For Autochambers, hyperbolic light response curves were fit for each plot on a monthly basis and gap filling occurred at the plot level. Gaps in nighttime NEE ($R_{eco}$, PAR < 10 μmol $m^{-2}$ $s^{-1}$ Tower and PAR < 5 μmol $m^{-2}$ $s^{-1}$ Autochamber) were filled using a summer season exponential temperature response with 10 cm soil temperature at Autochamber and air temperature at Tower (Text S1 and equation (S2)). The parameters obtained from the low PAR $R_{eco}$ model for each summer season were used to model daytime $R_{eco}$. Gross ecosystem primary productivity (GPP) was estimated by subtracting $R_{eco}$ from NEE.

#### 2.4.2. Nonsummer Gap Filling

Nonsummer season gap filling and cumulative $CO_2$ flux estimates were made separately for each shoulder season (fall and spring) and winter in order to account for small but detectable amounts of GPP in the autumn and spring. This method allows greater sensitivity to variation in growing season length and photosynthetic capacity (mosses and evergreens), rather than assuming the entire nonsummer season only consists of $R_{eco}$ [*Webb et al.*, 2016]. Tower measurements continued throughout the nonsummer season, and manual chamber measurements extended the data at Autochamber from October to November.

In the fall shoulder season, NEE and $R_{eco}$ at Autochamber were modeled using light and temperature response curves parameterized with weekly manual chamber measurements (equations (S1) and (S2)). In the spring shoulder season Autochamber GPP was estimated based on measured May GPP using Tower's ratio of early spring GPP to May GPP (equation (S4) and Text S1). $R_{eco}$ in spring was estimated using the winter model (equation (S3) and Text S1) for both Autochambers and Tower, because soils were typically still frozen and the area snow covered. NEE for spring was calculated as the sum of GPP and $R_{eco}$ (Text S1 and *Webb et al.* [2016]). At Tower, fall and spring were estimated weekly until GPP could no longer be detected.

Winter $R_{eco}$ fluxes were gap filled using an exponential relationship between Tower NEE, soil temperature (10 cm depth), and day of season (starting 1 October of each year) (equation (S3) and Text S1). Winter season $R_{eco}$ from 2008 to 2013 was modeled with a single parameter set from *Webb et al.* [2016], due to insufficient data coverage during individual years. In 2014, data coverage was greater and new model parameters were derived using soil temperature and day of season. Winter $R_{eco}$ for Autochamber was gap filled using the Tower parameters, but with plot-specific soil temperatures. Winter methods were evaluated in *Webb et al.* [2016].

All measured and gap filled 30 min $CO_2$ fluxes were aggregated to daily, seasonal, and yearly periods.

#### 2.4.3. Uncertainty Estimates

Uncertainties for Tower NEE were assessed using bootstrapping [*Liu et al.*, 2009]. Light response and temperature models were fit to measured data using seasonal resolution (summer and nonsummer) described above, and residuals were binned based on PAR (5 bins) for light response models and soil temperature (10 bins) for temperature models. In each bin category artificial data sets (1000) were created by adding predicted model values to randomly drawn and replaced residuals, and models were refit in order to gap fill data. The 95% confidence interval were obtained from 1000 complete flux time series for seasonal cumulative fluxes (see Text S2 for more details). Autochamber uncertainties were based on standard errors of replicate plot measurements ($n = 12$).

### 2.5. Data Analysis

Annual (October through September of the following year) NEE, GPP, and $R_{eco}$ were compared within a given year between the Tower and Autochamber methods using 95% confidence intervals generated from uncertainties. Differences were considered significant if the 95% confidence interval of the estimated aggregate fluxes did not overlap. Interannual differences in Autochamber fluxes were compared using an analysis of variance (ANOVA) and a post hoc Tukey test. Tower interannual differences were based on 95% confidence intervals generated from uncertainty analysis. The relationship of daily growing season NEE, GPP, and $R_{eco}$ were compared between Tower and mean Autochamber estimates for each year using linear regressions.

In order to determine whether ALT and WTD, two major physical drivers for this ecosystem, could explain variation in fluxes, we analyzed the relationship of summer season NEE, GPP, and $R_{eco}$ cumulative fluxes with ALT and WTD using a linear mixed effects model [*Bates et al.*, 2015]. Water table depth and ALT were fixed effects and method a random effect. We used a backward stepwise model selection to eliminate variables that resulted in less than five Akaike information criterion change (only WTD eliminated). All data processing and analyses were performed using the *R* platform [*R Development Core Team*, 2015] and a significance level of alpha = 0.05.

## 3. Results

### 3.1. Fluxes

#### 3.1.1. Net Ecosystem Exchange

On an annual basis, fluxes from both methods were a net $CO_2$ source during the 6 years with an average of $87 \pm 17$ g $CO_2$ C $m^{-2}$ $y^{-1}$ measured with Tower and $123 \pm 14$ g $CO_2$ C $m^{-2}$ $y^{-1}$ measured with Autochamber with a combined mean of $105 \pm 17$ g $CO_2$ C $m^{-2}$ $y^{-1}$. For the first 3 years Autochamber released significantly more $CO_2$ than Tower (Figure 1a and Table S2). Annual differences were driven by both summer and nonsummer season differences. During the nonsummer season, fluxes differed between methods in two of the 6 years with Autochamber having lower fluxes in the third year and higher NEE fluxes in the sixth year (Figure 1c). Over 6 years, the summer season sink strength increased significantly at Autochamber from almost neutral, $-7 \pm 7$, to a sink of $-105 \pm 11$ g $CO_2$ C $m^{-2}$ (Figures 2 and 1b and Table S2), reaching

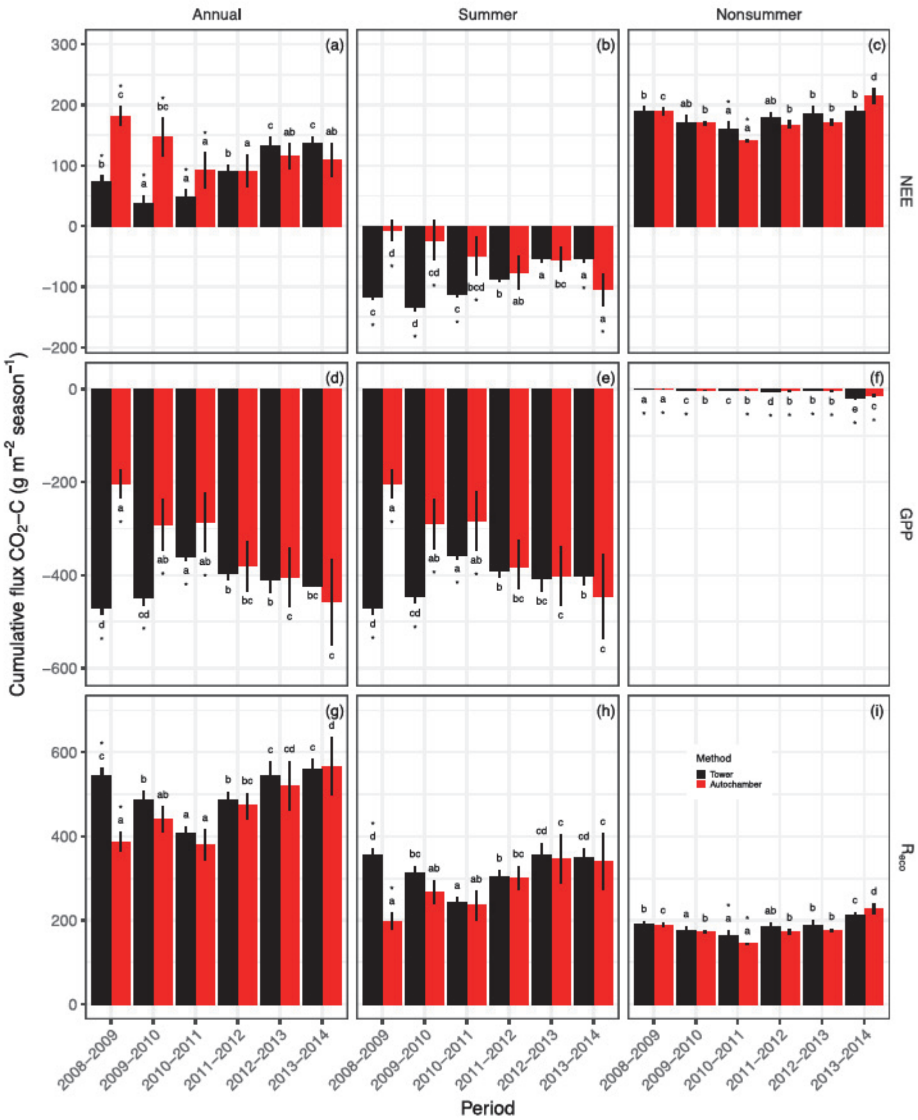


**Figure 1.** Annual, seasonal cumulative fluxes for the two methods (Tower black and Autochamber red) for each sampling period. (a–c) Net ecosystem exchange (NEE), (d–f) gross primary production (GPP), and (g–i) ecosystem respiration ($R_{eco}$). Note the difference in *y* axis scales for each flux and negative fluxes indicate carbon uptake. Means and 95% confidence intervals (Autochamber $n = 6$ and Tower $n = 1000$). Star (*) indicate significant differences within a period between methods. Different superscript letters indicate significant differences between periods ($p < 0.05$) within a method; Tower black bar and Autochamber red bars for each sampling period.

similar levels to those of the Tower. Tower NEE fluxes decreased over time, where net uptake decreased over time ranging from −134 g to −53 $CO_2$ C m$^{-2}$, with lowest net uptake during years five and six (Figures 2 and 1 and Table S2). Summer season NEE light response curves also indicated a progressive increase in C fixation at Autochamber, reaching similar parameters to Tower in the later years and surpassing it in the final year (Figures 3 and S2 and Table S3).

Daily NEE fluxes (measured and gap filled data) during the summer season were significantly correlated between Tower and Autochamber in all 6 ears (each year at least $p < 0.01$, $r^2 \geq 0.71$; Figures 4a to 4f). As the years progressed, the fluxes became more similar to each other in magnitude (Figures 4a and 4f) and the slope approached 1 (2009 slope = 0.35 and 2014 slope = 0.99). Comparing methods using only measured data, when both were sampled in the same half-hourly period, found that the direction of NEE (i.e., $CO_2$ source or sink) was similar 79–86% of the time, and methods became more similar over time. When considering the transition point from sink to source, the date when cumulative NEE became positive was similar for

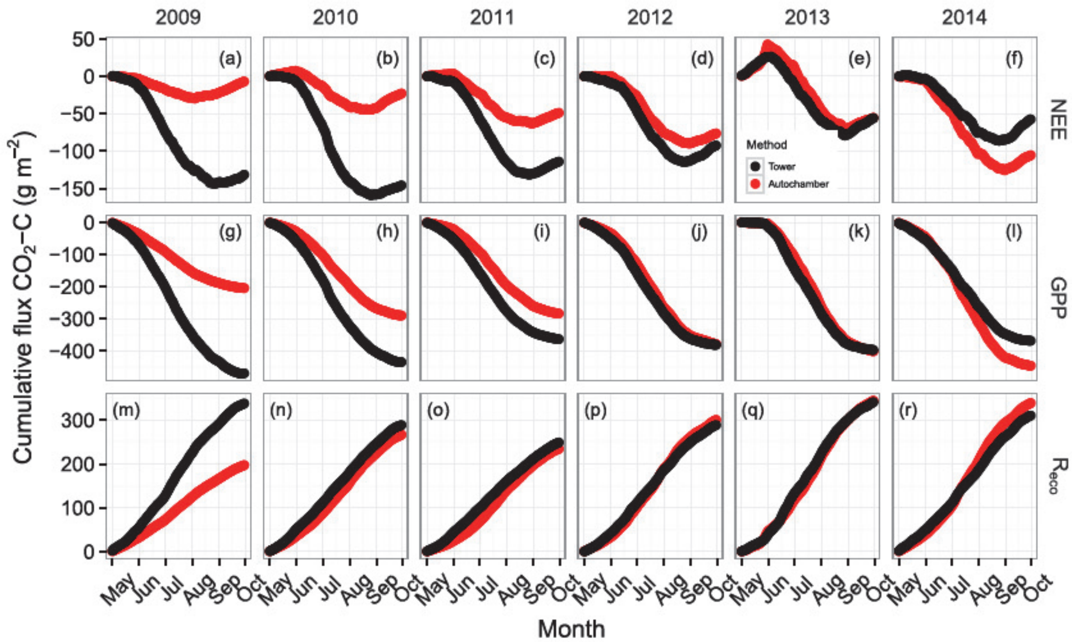


**Figure 2.** Summer season (1 May to 30 September, except 2013 stared 1 June) mean daily cumulative fluxes for the two methods (Tower black symbols and Autochamber red symbols). (a–f) Net ecosystem exchange (NEE), (g–l) gross primary production (GPP), and (m–r) ecosystem respiration ($R_{eco}$). Note the difference in *y* axis scales for each flux; negative fluxes indicate C uptake.

Tower and Autochamber and occurred between 25 August and 30 August, only a 6 day range across five of the 6 years. The transition between sink and source was consistent despite interannual variation in spring snowmelt, which varied on average 12 days over the 6 years (Table 1). The first year of observation, 2009, was an exception; Autochamber NEE changed from a net $CO_2$ sink to a source on 4 August was 22 days earlier than the other years (Table 2). In contrast the Tower switched on 27 August 2009, consistent with all other years.

### 3.1.2. Gross Primary Production

Daily GPP was significantly correlated between methods during all 5 years (each year at least $p < 0.01$, $r^2 \geq 0.77$; Figures 4g to 4i). Annual GPP was lower during the first 3 years at Autochamber than at Tower, with the magnitude of the difference dropping by almost half in each subsequent year (Figure 1d Table S2). Tower GPP uptake was greatest in the first year of measurement (−471 g $CO_2$ C $m^{-2}$) and then decreased to a relatively consistent level by the third year (−396 to −423 g $CO_2$ C $m^{-2}$). In contrast, Autochamber showed a progressive increase over time (Figure 1d), such that GPP was small during the first year (−205 g $CO_2$ C $m^{-2}$) but increased by ~100 g $CO_2$ C$m^{-2}$ in the second year, held that increase in the third year, and then increased again in years four (~180 $CO_2$ C $m^{-2}$ more than the first year), five (~200 $CO_2$ C $m^{-2}$ more than the first year), and six (~250 $CO_2$ C $m^{-2}$ more than the first year; Figures 2 and 1d and Table S2). The Autochamber increase over time was driven by increased GPP in June, July, and August of each year (Figure S2 and Table S3). Summer season GPP had similar trends to annual GPP (Figures 2 and 1e and Table S2). Nonsummer season contributed relatively little to annual GPP (−0.4 to −21 g $CO_2$ C $m^{-2}$ both methods) and showed an increase with both methods over time (Figure 1f and Table S2). Autochamber had a significantly lower uptake in four of the 6 years compared to Tower (Table S2) for nonsummer season.

### 3.1.3. Ecosystem Respiration

Daily $R_{eco}$ was significantly correlated between methods during all 6 years (each year at least $p < 0.01$, $r^2 \geq 0.44$; Figures 4m to 4r). Annual $R_{eco}$ was significantly lower in Autochamber during the first year (Autochamber: 387 g $CO_2$ C $m^{-2}$ Tower: 545 g $CO_2$ C $m^{-2}$; Figure 1g and Table S2). After 2009 Autochamber $R_{eco}$ and Tower were well correlated with no observable trend over time. Summer season $R_{eco}$ trends were similar to annual fluxes. Tower $R_{eco}$ ranged from 302 to 355 g $CO_2$ C $m^{-2}$ and Autochamber $R_{eco}$ 198 to 347 g $CO_2$ C $m^{-2}$ (Figures 2 and 1h and Table S2). During the summer season $R_{eco}$ and GPP were tightly coupled in both methods, with

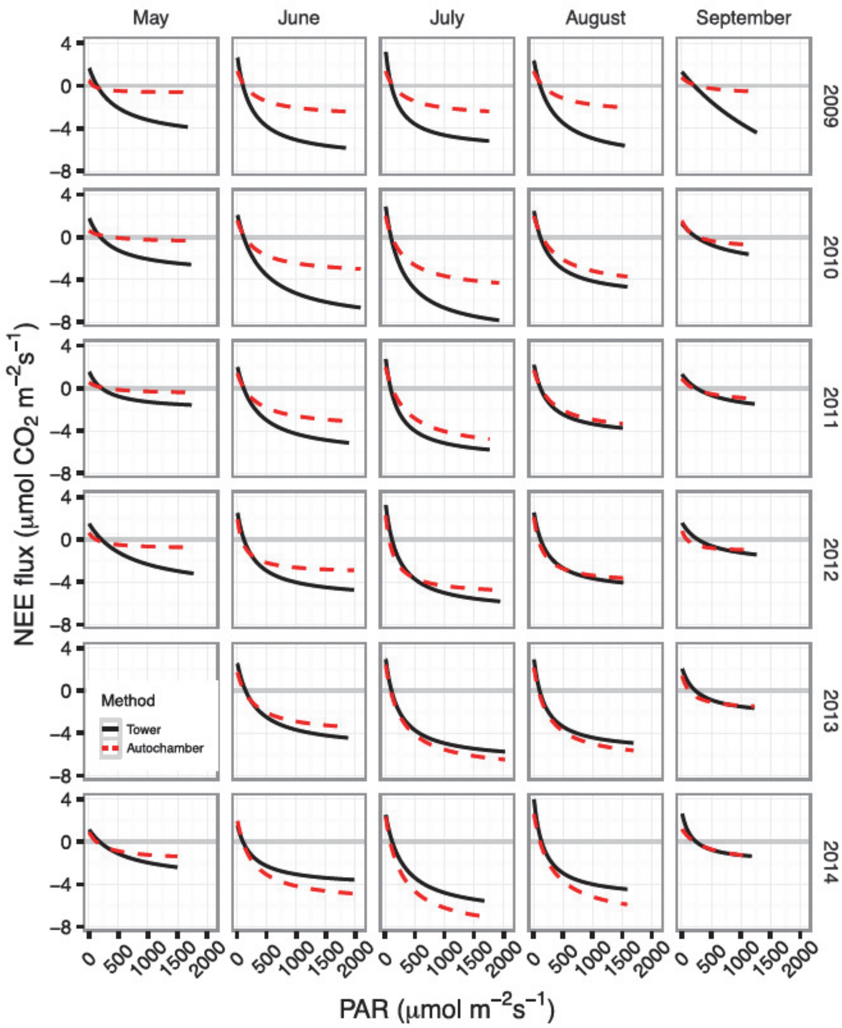


**Figure 3.** Summer season monthly modeled light response curves for Tower (black solid lines) and Autochamber methods (red dashed lines). May 2013 contains no data for Autochamber and Tower was excluded. For more model information see equation (1) in supporting information Text S1 and model parameters estimates Table S3.

high seasonal cumulative GPP occurring during periods with high seasonal cumulative $R_{eco}$. The ratio of $R_{eco}$/GPP for the summer season was consistent between years, where Tower was on average 0.77 and Autochamber 0.84 (Table S6). Nonsummer season $R_{eco}$ with Tower was 163 to 211 g $CO_2$ C $m^{-2}$ and 144 to 228 g $CO_2$ C $m^{-2}$ with Autochamber, which accounts for 37% and 39% of annual respiration fluxes, respectively (Figures 1g and 1i and Table S2).

### 3.2. Fluxes and Environmental Factors

Summer season active layer thickness was significantly shallower with Autochamber for the first 2 years than with Tower ($p < 0.001$; Figure S1). There was a significant relationship ($p < 0.01$, Figure 5 and Table S7) between summer season fluxes (NEE, GPP, and $R_{eco}$) and active layer thickness (ALT). GPP had a stronger relationship with ALT ($r^2 = 0.84$, Figure 5b; higher $CO_2$ uptake increased with greater ALT) than $R_{eco}$ ($r^2 = 0.59$; Figure 5c and Table S7), followed by NEE (Figure 5a and Table S7). There was no relationship between fluxes and WTD (Table S7).

## 4. Discussion

Annual $CO_2$ fluxes were consistent in demonstrating that the tundra ecosystem was a net annual source of $CO_2$ to the atmosphere (mean 105 ± 17 g $CO_2$ C $m^{-2}$ $y^{-1}$ across methods and years) during our study

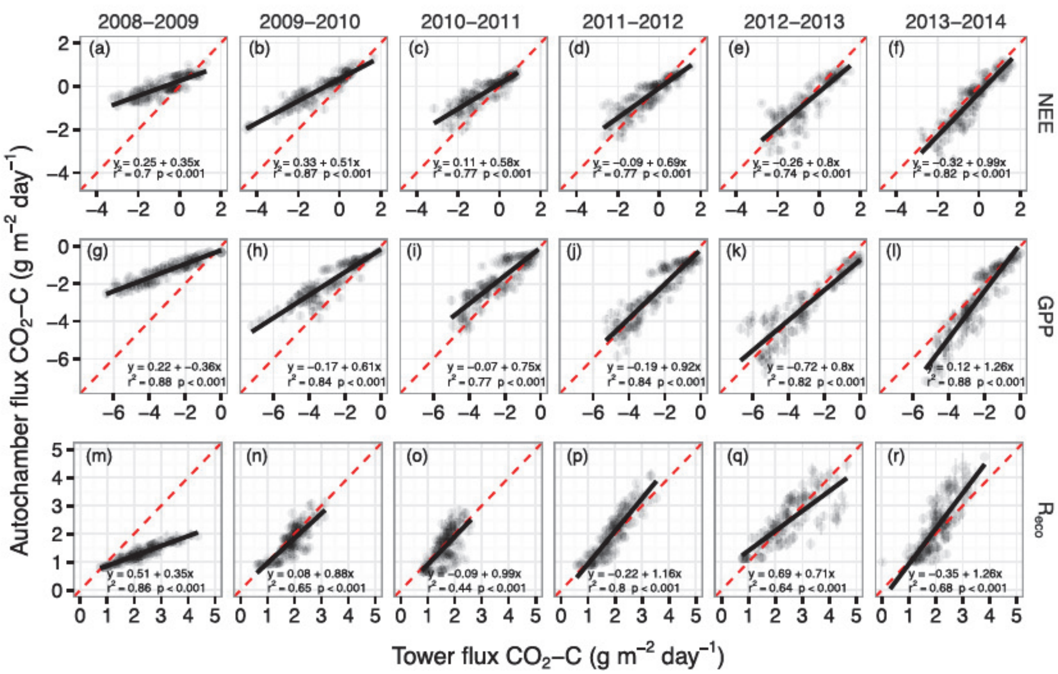


**Figure 4.** (a–f) Daily fluxes of net ecosystem exchange (NEE), (g–l) gross primary production (GPP), and (m–r) ecosystem respiration ($R_{eco}$) for each summer season (1 May to 30 September, except 2013 stared 1 June) for the two methods (Tower and Autochamber). Autochamber means and standard errors are based on fence replicates ($n$ = 6). The black line represents linear regression and the red dashed line the one-to-one line. Negative fluxes indicate C uptake.

period. Our Tower measurements (87 ± 17 g $CO_2$ C m$^{-2}$ y$^{-1}$) were higher than other eddy covariance studies, which have reported annual tundra $CO_2$ fluxes that vary from −6.4 to 68.7 g $CO_2$ C m$^{-2}$ y$^{-1}$ [*Euskirchen et al.*, 2012; *Belshe et al.*, 2013; *Lüers et al.*, 2014; *Oechel et al.*, 2014; *Zona et al.*, 2014]. Autochamber measurements (123 ± 14 g $CO_2$ C m$^{-2}$ y$^{-1}$) were within the range of other studies, which have reported annual fluxes from the tundra between −109 and 194 g $CO_2$ C m$^{-2}$ y$^{-1}$—chamber measurements [*Grogan and Iii*, 1999; *Trucco et al.*, 2012; *Kim et al.*, 2016].

Active layer thickness was identified as a key driver of cumulative GPP, NEE, and $R_{eco}$ throughout the summer season and explained differences between Tower and Autochambers in the first 2 years. Increased GPP and $R_{eco}$ were related to deeper thaw, which is similar to other studies at EML [*Vogel et al.*, 2009; *Trucco et al.*, 2012]. Increased plant productivity as a result of active layer deepening is associated with increased nutrient availability as permafrost thaws [*Finger et al.*, 2016; *Salmon et al.*, 2016], although autotrophic respiration also increases [*Hicks Pries et al.*, 2015]. Active layer thickness incorporates several characteristics of the soil environment including soil moisture, soil structure, and soil temperature [*Trucco et al.*, 2012].

**Table 1.** Mean Air Temperatures, Total Annual Precipitation (Rainfall), Cumulative Photosynthetic Active Radiation (PAR), Soil Active Layer Thickness, Water Table Depths, and Snowmelt Date at Eight Mile Lake, Healy Alaska, USA[a]

| Season (Year of Study) | Temperature (°C) Annual | Summer Season | Nonsummer Season | Annual Rainfall (mm) | Summer Season Cumulative PAR (Mole/m$^2$) | Active Layer Thickness (cm) Tower | Autochamber | Water Table Depth (cm) Tower | Autochamber | Snowmelt (Date) |
|---|---|---|---|---|---|---|---|---|---|---|
| 2008–2009 (1) | −3.4 | 9.7 | −12.8 | 178.2 | 4991.7 | 67.6 (2.5) | 55.4 (0.8) | 18.5 (2.0) | 27.6 (0.7) | NA |
| 2009–2010 (2) | −1.2 | 9.8 | −9.2 | 249.8 | 4794.9 | 69.9 (1.9) | 58.3 (0.7) | 14.8 (2.3) | 20.3 (0.3) | 2010-04-27 |
| 2010–2011 (3) | −3.2 | 8.3 | −11.5 | 164.4 | 5193.2 | 60.0 (1.6) | 56.4 (0.9) | 15.1 (2.3) | 23.8 (0.3) | 2011-04-27 |
| 2011–2012 (4) | −3.3 | 9.1 | −12.1 | 223.4 | 4855.3 | 65.3 (1.2) | 60.9 (0.7) | 17.3 (2.0) | 22.1 (0.3) | 2012-05-04 |
| 2012–2013 (5) | −4.1 | 9.3 | −13.7 | 167.2 | 5502.3 | 66.3 (1.9) | 62.8 (1.2) | 23.6 (1.6) | 23.8 (0.4) | 2013-05-27 |
| 2013–2014 (6) | −0.9 | 9.1 | −8.2 | 312.2 | 4553.4 | 61.1 (1.9) | 65.3 (1.6) | 10.4 (1.9) | 14.5 (0.7) | 2014-04-21 |
| Mean (SE) | −2.7 (0.5) | 9.2 (0.2) | −11.3 (0.9) | 215.9 (23.8) | 4981.8 (135.4) | 65.0 (1.6) | 59.9 (1.6) | 16.6 (1.8) | 22.0 (1.8) | |

[a]Summer season data represents the period from 1 May to 30 September and nonsummer season 1 October to 30 April of the following year.

**Table 2.** The Date of First Change From Observed Summer Season Ecosystem $CO_2$ Net Uptake to a Net Source of $CO_2$[a]

| Tower | Autochamber |
|---|---|
| 27-AUG-2009 | 04-AUG-2009 |
| 26-AUG-2010 | 26-AUG-2010 |
| 27-AUG-2011 | 30-AUG-2011 |
| 25-AUG-2012 | 29-AUG-2012 |
| 28-AUG-2013 | 28-AUG-2013 |
| 24-AUG-2014 | 31-AUG-2014 |

[a]Date (dd-AUG-yyyy).

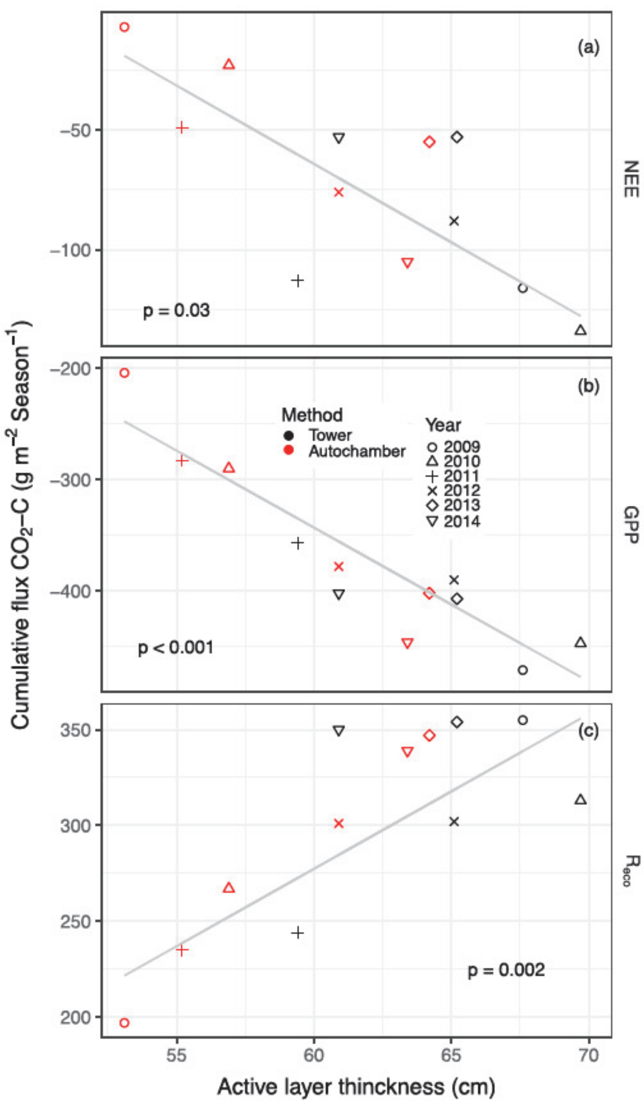


**Figure 5.** The relationship of summer season (1 May to 30 September) cumulative fluxes with active layer thickness (ALT) for the two methods (Tower black symbols and Autochamber red symbols). *P* values denote significant slope parameters (Tables S7). (a) NEE is net ecosystem exchange, (b) GPP is gross primary production, and (c) Reco is Ecosystem respiration. Negative fluxes indicate $CO_2$ uptake. Note the difference in *y* axis scales for each flux.

Increased ALT was also related to increases in $R_{eco}$ by stimulating heterotrophic respiration as a result of increased organic matter decomposition under higher temperatures and increased moisture [*Hicks Pries et al.*, 2013b], and the availability of deep soil C [*Schuur et al.*, 2009; *Hicks Pries et al.*, 2013a; *Koven et al.*, 2015].

Summer season daily fluxes of NEE, GPP, and $R_{eco}$ were correlated between Autochamber and Tower, with $R_{eco}$ showing less correlation and more variability between methods, consistent with other tundra sites that compared these two types of measurement methods [*Zamolodchikov et al.*, 2003; *Kade et al.*, 2012]. Even though daily GPP and NEE fluxes were highly correlated between methods, they differed in magnitude for the first 3 years; Autochamber measurements had lower uptake for the first 3 years. This is contrary to what has been observed by other studies comparing chambers and eddy covariance, which have shown higher net $CO_2$ uptake from chamber measurements [*Fox et al.*, 2008; *Kade et al.*, 2012]. The discrepancy between Tower and Autochamber in magnitude of NEE, GPP, and $R_{eco}$ and light sensitivity model parameters (Table S3) in the initial years may have derived from the unintended effects of experimental setup of the Autochamber system. Chamber bases for autochamber measurements were installed to a depth of 5–8 cm, which may have severed rooting systems and reduced fine root respiration [*Wang et al.*, 2005; *Heinemeyer et al.*, 2011]. In Arctic plant communities, belowground biomass is concentrated near the surface [*Sullivan and Welker*, 2005; *Sullivan et al.*, 2007; *Iversen et al.*, 2015], and stored root C and respiration can contribute substantially to C flux dynamics [*Hopkins et al.*, 2013; *Cahoon et al.*, 2016]. Fine root production also coincides with whole plant belowground allocation of C resources and reserves [*Olsrud and Christensen*, 2004]. Any alteration to belowground resources can therefore affect plant seasonal responses aboveground and belowground. Autochamber was dominated by the tussock-forming sedge *Eriophorum*, which has a quick fine root turnover rate of ~1 year [*Shaver and Billings*, 1975] and has a late summer season growth pulse of fine roots [*Kummerow and Russell*, 1980; *Shaver et al.*, 1986; *Cahoon et al.*, 2016]. We observed a reduction in $R_{eco}$ during the first year only at Autochamber when compared to Tower fluxes. The severing of *Eriophorum* roots and/or root disturbance during installation in the autumn prior to measurements could have delayed production of fine roots in the following season (year one of this study), which would have altered fine root litter inputs during that year and might explain the low $R_{eco}$ during that year. Fine root decomposition accounts for a large proportion of respiration inputs to tundra soil [*Loya et al.*, 2004]. Not only was $R_{eco}$ lower during the first year for Autochamber, but GPP was also lower and the ecosystem became a net source of $CO_2$ earlier in the summer season than any other year (Table S2). The use of reserves for root growth and/or repair or access to spring nutrients could compromise summer plant performance for the first 3 years. Although summer season NEE was significantly different in the sixth year, GPP and $R_{eco}$ were similar between methods.

Interannual NEE variability can be influenced by environmental factors that determine the start and end of the summer season. The timing of snowmelt plays an important role for determining the annual $CO_2$ balance for the Arctic [*Aurela et al.*, 2004; *Lund et al.*, 2012], and late snowmelt can delay phenology [*Ernakovich et al.*, 2014] resulting in lower annual NEE but can vary depending on vegetation type [*Humphreys and Lafleur*, 2011]. *Mbufong et al.* [2014] found that tundra peak productivity in July was unrelated to the start of the summer season and in fact $R_{eco}$ was a stronger driver of interannual NEE flux variability than the timing of growing season start. In our study, snowmelt in the fifth year (2013) of monitoring at Tower and Autochamber was exceptionally late in comparison with other years (Table 1), yet that year did not have the lowest summer season NEE uptake. The low GPP during the month of May in 2013 was compensated for by increased carbon fixation in the following months. This indicates that tundra plants are capable of reaching high productivity by upregulating photosynthesis [*Bosiö et al.*, 2014] in a short period of time (Table S3 and Figure 3). Other environmental drivers of respiration such as temperature and moisture play an important role in the net $CO_2$ balance of the season [*Euskirchen et al.*, 2012] such as increased temperatures can offset ecosystem uptake by increased respiration late in the summer season, but respiration can also be inhibited by increases in precipitation as decomposition is slowed down under wet conditions.

Autochamber and Tower methods were remarkably consistent in capturing biological down regulation of ecosystem productivity and becoming a net source of $CO_2$ within a small window in August, regardless of the start of the summer season. This down regulation was likely due to the onset of senescence, which is thought to be regulated mostly by photoperiod in tundra plants [*Shaver and Kummerow*, 1992].

Nonsummer season fluxes accounted for approximately 30% of the $CO_2$ released annually, which is within the upper range of annual budgets in other studies (10–30%) [*Fahnestock et al.*, 1998; *Grogan and Iii*, 1999; *Elberling*, 2007; *Kim et al.*, 2016]; like in other studies that estimate annual Arctic $CO_2$ flux, nonsummer losses offset the summer season gains [*Fahnestock et al.*, 1998; *Vogel et al.*, 2009; *Euskirchen et al.*, 2012; *Lüers et al.*, 2014; *Oechel et al.*, 2014]. Nonsummer C flux estimates have many challenges and large uncertainty: direct measurements are difficult to obtain [*Goodrich et al.*, 2016] and the differences between nonsummer measurement methods can be greater than the estimates of interannual variation in $CO_2$ fluxes [*Björkman et al.*, 2010; *Webb et al.*, 2016]. In our study, nonsummer season fluxes were calculated from values that were 11% measured and 89% modeled (Table S1) for the whole study period (both Tower and Autochamber used the same data set), which meant model parameterization was limited to a small quantity of data. *Goodrich et al.* [2016] reported similar coverage during the winter using same type of $CO_2$ analyzer. Despite our small and sporadic data set, our nonsummer measurements span the entire nonsummer season and our model builds on extensive examination of winter fluxes done by *Webb et al.* [2016]. Our results represent further evidence of the influence of nonsummer season $CO_2$ fluxes to annual C budgets from a subarctic site, which is in line with other studies throughout the Arctic [*Oechel et al.*, 1997; *Fahnestock et al.*, 1999; *Jones et al.*, 1999; *Welker et al.*, 2000; *Schimel et al.*, 2006; *Sullivan et al.*, 2008; *Grogan*, 2012; *Cooper*, 2014]. As we improve our data collection during winter, we will be able to evaluate more precisely the mechanisms driving ecosystem $CO_2$ loss during this time of the year to better estimate our annual budgets of carbon.

## 5. Conclusion

Our $CO_2$ flux measurements show that during 6 years of measurement the tundra ecosystem was a consistent annual net source of $CO_2$ to the atmosphere (105 ± 17 g $CO_2$ C $m^{-2}$). While this ecosystem was a $CO_2$ sink during the summer, $CO_2$ emissions during the nonsummer months offset summer $CO_2$ uptake in every year. Active layer thickness was a significant driver of GPP, likely as a result of increased nutrient availability with deeper thaw and also increased $R_{eco}$ at both landscape and plot scales. Differences between fluxes at Tower and Autochamber in the first year could be related to the impact of experimental setup, and the severing of roots. This highlights the need for long-term experiments in order to make generalizations about $CO_2$ flux dynamics and sensitivity to environmental drivers. Further research evaluating the coupling of belowground and aboveground dynamics, and the relationship between summer and nonsummer processes is needed to further our understanding of tundra C cycle dynamics and potential implications in the face of climate change.

**Acknowledgments**
This work was made possible by assistance from researchers and technicians of Bonanza Creek LTER and from the Schuur lab (Meghan Taylor, Elaine Pegoraro, Chris Ebert, César Plaza, Justin Ledman, Catherine Johnson, Peter Ganzlin, Camilo Mojica, and John Krapek). This work was funded by NSF CAREER Program, NSF Bonanza Creek LTER Program, Department of Energy NICCR Program (E.A.G.S.), TES (E.A.G.S.), the U.S. National Parks and Inventory Monitoring Program (E.A.G.S.), and NSF OPP (S.M.N.). Data presented in this paper are archived at Bonanza Creek LTER Data Catalog and can be accessed through their database tool: http://www.lter.uaf.edu/data/data-catalog.

## References

Aubinet, M., et al. (2000), Estimates of the annual net carbon and water exchange of forests: The EUROFLUX methodology, *Adv. Ecol. Res.*, *30*(30), 113–175.

Aurela, M., T. Laurila, and J. P. Tuovinen (2004), The timing of snow melt controls the annual $CO_2$ balance in a subarctic fen, *Geophys. Res. Lett.*, *31*, L16119, doi:10.1029/2004GL020315.

Bates, D., M. Mächler, B. Bolker, and S. Walker (2015), Fitting linear mixed-effects models using lme4, *J. Stat. Softw.*, *67*(1), 1–48, doi:10.18637/jss.v067.i01.

Belshe, E. F., E. A. G. Schuur, and B. M. Bolker (2012), Incorporating spatial heterogeneity created by permafrost thaw into a landscape carbon estimate, *J. Geophys. Res.*, *117*, G01026, doi:10.1029/2011JG001836.

Belshe, E. F., E. A. G. Schuur, and B. M. Bolker (2013), Tundra ecosystems observed to be $CO_2$ sources due to differential amplification of the carbon cycle, *Ecol. Lett.*, *16*(10), 1307–1315, doi:10.1111/ele.12164.

Björkman, M. P., E. Morgner, and E. J. Cooper (2010), Winter carbon dioxide effluxes from Arctic ecosystems: An overview and comparison of methodologies, *Global Biogeochem. Cycles*, *24*, GB3010, doi:10.1029/2009GB003667.

Blanc-Betes, E., J. M. Welker, N. C. Sturchio, J. P. Chanton, and M. A. Gonzalez-Meler (2016), Winter precipitation and snow accumulation drive the methane sink or source strength of Arctic tussock tundra, *Global Change Biol.*, *22*(8), 2818–2833, doi:10.1111/gcb.13242.

Bosiö, J., C. Stiegler, M. Johansson, and H. N. Mbufong (2014), Increased photosynthesis compensates for shorter growing season in subarctic tundra—8 years of snow accumulation manipulations, *Clim. Change*, *127*, 321–334, doi:10.1007/s10584-014-1247-4.

Burba, G. G., D. K. McDermitt, A. Grelle, D. J. Anderson, and L. Xu (2008), Addressing the influence of instrument surface heat exchange on the measurements of $CO_2$ flux from open-path gas analyzers, *Global Change Biol.*, *14*(8), 1854–1876, doi:10.1111/j.1365-2486.2008.01606.x.

Cahoon, S., P. F. Sullivan, C. Gamm, J. M. Welker, D. Eissenstat, and E. Post (2016), Limited variation in proportional contributions of auto-and heterotrophic soil respiration, despite large differences in vegetation structure and function in the Low Arctic, *Biogeochemistry*, *179*, 339–351, doi:10.1007/s10533-016-0184-x.

Chapin, F. S., and G. R. Shaver (1985), Individualistic growth-response of tundra plant-species to environmental manipulations in the field, *Ecology*, *66*(2), 564–576.

Cooper, E. J. (2014), Warmer shorter winters disrupt Arctic terrestrial ecosystems, *Annu. Rev. Ecol. Evol. Syst.*, *45*, 271–295, doi:10.1146/annurev-ecolsys-120213-091620.

Davidson, E. A., and I. A. Janssens (2006), Temperature sensitivity of soil carbon decomposition and feedbacks to climate change, *Nature*, *440*(7081), 165–173, doi:10.1038/nature04514.

DeMarco, J., M. C. Mack, M. S. Bret-Harte, M. Burton, and G. R. Shaver (2014), Long-term experimental warming and nutrient additions increase productivity in tall deciduous shrub tundra, *Ecosphere*, *5*(6), 72, doi:10.1890/ES13-00281.1.

Elberling, B. (2007), Annual soil $CO_2$ effluxes in the High Arctic: The role of snow thickness and vegetation type, *Soil Biol. Biochem.*, *39*(2), 646–654, doi:10.1016/j.soilbio.2006.09.017.

Epstein, H. E., M. K. Raynolds, and D. A. Walker (2012), Dynamics of aboveground phytomass of the circumpolar Arctic tundra during the past three decades, *Environ. Res. Lett.*, *7*, 12, doi:10.1088/1748-9326/7/1/015506.

Ernakovich, J. G., K. A. Hopping, A. B. Berdanier, R. T. Simpson, E. J. Kachergis, H. Steltzer, and M. D. Wallenstein (2014), Predicted responses of arctic and alpine ecosystems to altered seasonality under climate change, *Global Change Biol.*, *20*(10), 3256–3269, doi:10.1111/gcb.12568.

Euskirchen, E. S., A. D. McGuire, and T. S. Rupp (2009), Projected changes in atmospheric heating due to changes in fire disturbance and the snow season in the western Arctic, 2003–2100, *J. Geophys. Res.*, *114*, G04022, doi:10.1029/2009JG001095.

Euskirchen, E. S., M. S. Bret-Harte, G. J. Scott, C. Edgar, and G. R. Shaver (2012), Seasonal patterns of carbon dioxide and water fluxes in three representative tundra ecosystems in northern Alaska, *Ecosphere*, *3*(1), 4, doi:10.1890/ES11-00202.1.

Fahnestock, J. T., M. H. Jones, and J. M. Welker (1999), Wintertime $CO_2$ efflux from arctic soils: Implications for annual carbon budgets, *Global Biogeochem. Cycles*, *13*(3), 775–779.

Fahnestock, J. T., M. H. Jones, P. D. Brooks, D. A. Walker, and J. M. Welker (1998), Winter and early spring $CO_2$ efflux from tundra communities of northern Alaska, *J. Geophys. Res.*, *103*(D22), 29023–29027.

Finger, R. A., M. R. Turetsky, K. Kielland, R. W. Ruess, M. C. Mack, and E. S. Euskirchen (2016), Effects of permafrost thaw on nitrogen availability and plant–soil interactions in a boreal Alaskan lowland, edited by N. Wurzburger, *J. Ecol.*, *104*(6), 1542–1554, doi:10.1111/1365-2745.12639.

Foken, T., and B. Wichura (1996), Tools for quality assessment of surface-based flux measurements, *Agric. For. Meteorol.*, *78*(1–2), 83–105.

Fox, A. M., B. Huntley, C. R. Lloyd, M. Williams, and R. Baxter (2008), Net ecosystem exchange over heterogeneous Arctic tundra: Scaling between chamber and eddy covariance measurements, *Global Biogeochem. Cycles*, *22*, GB2027, doi:10.1029/2007GB003027.

Geml, J., T. A. Semenova, L. N. Morgado, and J. M. Welker (2016), Changes in composition and abundance of functional groups of arctic fungi in response to long-term summer warming, *Biol. Lett.*, *12*(11), 20160503, doi:10.1098/rsbl.2016.0503.

Goodrich, J. P., W. C. Oechel, B. Gioli, V. Moreaux, P. C. Murphy, G. Burba, and D. Zona (2016), Impact of different eddy covariance sensors, site set-up, and maintenance on the annual balance of $CO_2$ and $CH_4$ in the harsh Arctic environment, *Agric. For. Meteorol.*, *228*, 239–251, doi:10.1016/j.agrformet.2016.07.008.
Goulden, M., J. Munger, S. Fan, B. Daube, and S. Wofsy (1996), Measurements of carbon sequestration by long-term eddy covariance: Methods and a critical evaluation of accuracy, *Global Change Biol.*, *2*, 169–182, doi:10.1111/j.1365-2486.1996.tb00070.x.
Groendahl, L., T. Friborg, and H. Soegaard (2007), Temperature and snow-melt controls on interannual variability in carbon exchange in the high Arctic, *Theor. Appl. Climatol.*, *88*(1–2), 111–125, doi:10.1007/s00704-005-0228-y.
Grogan, P. (2012), Cold season respiration across a low Arctic landscape: The influence of vegetation type, snow depth, and interannual climatic variation, *Arct. Antarct. Alp. Res.*, *44*, 446–456, doi:10.1657/1938-4246-44.4.446.
Grogan, P., and F. C. Iii (1999), Arctic soil respiration: Effects of climate and vegetation depend on season, *Ecosystems*, *2*, 451–459.
Heinemeyer, A., C. Di Bene, A. R. Lloyd, D. Tortorella, R. Baxter, B. Huntley, A. Gelsomino, and P. Ineson (2011), Soil respiration: Implications of the plant-soil continuum and respiration chamber collar-insertion depth on measurement and modelling of soil $CO_2$ efflux rates in three ecosystems, *Eur. J. Soil Sci.*, *62*(1), 82–94, doi:10.1111/j.1365-2389.2010.01331.x.
Henry, G., and U. Molau (1997), Tundra plants and climate change: The International Tundra Experiment (ITEX), *Global Change Biol.*, *3*, 1–9.
Hicks Pries, C. E., E. A. G. Schuur, and K. G. Crummer (2013a), Thawing permafrost increases old soil and autotrophic respiration in tundra: Partitioning ecosystem respiration using $\delta^{13}C$ and $\Delta^{14}C$, *Global Change Biol.*, *19*, 649–661, doi:10.1111/gcb.12058.
Hicks Pries, C. E., E. A. G. Schuur, J. G. Vogel, and S. M. Natali (2013b), Moisture drives surface decomposition in thawing tundra, *J. Geophys. Res. Biogeosci.*, *118*, 1133–1143, doi:10.1002/jgrg.20089.
Hicks Pries, C. E., R. S. P. van Logtestjin, E. A. G. Schuur, S. M. Natali, J. H. C. Cornelissen, R. Aerts, and E. Dorrepaal (2015), Decadal warming causes a consistent and persistent shift from heterotrophic to autotrophic respiration in contrasting permafrost ecosystems, *Global Change Biol.*, *21*, 4508–4519, doi:10.1111/gcb.13032.
Hollister, R. D., J. L. May, K. S. Kremers, C. E. Tweedie, S. F. Oberbauer, J. A. Liebig, T. F. Botting, R. T. Barrett, and J. L. Gregory (2015), Warming experiments elucidate the drivers of observed directional changes in tundra vegetation, *Ecol. Evol.*, *5*(9), 1881–1895, doi:10.1002/ece3.1499.
Hopkins, F., M. A. Gonzalez-Meler, C. E. Flower, D. J. Lynch, C. Czimczik, J. Tang, and J.-A. Subke (2013), Ecosystem-level controls on root-rhizosphere respiration, *New Phytol.*, *199*(2), 339–351, doi:10.1111/nph.12271.
Hugelius, G., et al. (2014), Estimated stocks of circumpolar permafrost carbon with quantified uncertainty ranges and identified data gaps, *Biogeosciences*, *11*(23), 6573–6593, doi:10.5194/bg-11-6573-2014-supplement.
Humphreys, E. R., and P. M. Lafleur (2011), Does earlier snowmelt lead to greater $CO_2$ sequestration in two low Arctic tundra ecosystems?, *Geophys. Res. Lett.*, *38*, doi:10.1029/2011GL047339.
International Panel on Climate Change (IPCC) (2014), *Climate Change 2013—The Physical Science Basis*, pp. 467–553; 1219–1256, Cambridge Univ. Press, New York.
Iversen, C. M., V. L. Sloan, P. F. Sullivan, E. S. Euskirchen, A. D. McGuire, R. J. Norby, A. P. Walker, J. M. Warren, and S. D. Wullschleger (2015), The unseen iceberg: Plant roots in Arctic tundra, *New Phytol.*, *205*(1), 34–58, doi:10.1111/nph.13003.
Jones, M. H., J. T. Fahnestock, and J. M. Welker (1999), Early and late winter $CO_2$ efflux from arctic tundra in the Kuparuk River watershed, Alaska, USA, *Arct. Antarct. Alp. Res.*, *31*(2), 187–190.
Kade, A., M. S. Bret-Harte, E. S. Euskirchen, C. Edgar, and R. A. Fulweber (2012), Upscaling of $CO_2$ fluxes from heterogeneous tundra plant communities in Arctic Alaska, *J. Geophys. Res.*, *117*, G04007, doi:10.1029/2012JG002065.
Kelsey, K. C., A. J. Leffler, and K. H. Beard (2016), Interactions among vegetation, climate, and herbivory control greenhouse gas fluxes in a subarctic coastal wetland, *J. Geophys. Res. Biogeosci.*, *121*, 2960–2975, doi:10.1002/2016JG003546.
Kim, Y., S.-J. Park, B.-Y. Lee, and D. Risk (2016), Continuous measurement of soil carbon efflux with Forced Diffusion (FD) chambers in a tundra ecosystem of Alaska, *Sci. Total Environ.*, *566-567*, 175–184, doi:10.1016/j.scitotenv.2016.05.052.
Kormann, R., and F. X. Meixner (2001), An analytical footprint model for non-neutral stratification, *Boundary Layer Meteorol.*, *99*, 207–224.
Koven, C. D., B. Ringeval, P. Friedlingstein, P. Ciais, P. Cadule, D. Khvorostyanov, G. Krinner, and C. Tarnocai (2011), Permafrost carbon-climate feedbacks accelerate global warming, *Proc. Natl. Acad. Sci. U.S.A.*, *108*(36), 14769–14774, doi:10.1073/pnas.1103910108.
Koven, C. D., D. M. Lawrence, and W. J. Riley (2015), Permafrost carbon-climate feedback is sensitive to deep soil carbon decomposability but not deep soil nitrogen dynamics, *Proc. Natl. Acad. Sci. U.S.A.*, *112*(12), 3752–3757, doi:10.1073/pnas.1415123112.
Kummerow, J., and M. Russell (1980), Seasonal root growth in the Arctic tussock tundra, *Oecologia*, *47*(2), 196–199.
Lee, H., E. A. G. Schuur, and J. G. Vogel (2010), Soil $CO_2$ production in upland tundra where permafrost is thawing, *J. Geophys. Res.*, *115*, G01009, doi:10.1029/2008JG000906.
Lee, H., E. A. G. Schuur, J. G. Vogel, and M. Lavoie (2011), A spatially explicit analysis to extrapolate carbon fluxes in upland tundra where permafrost is thawing, *Global Change Biol.*, *17*, 1379–1393, doi:10.1111/j.1365-2486.2010.02287.x.
Liu, M., H. L. He, G. R. Yu, Y. Q. Luo, and X. M. Sun (2009), Uncertainty analysis of $CO_2$ flux components in subtropical evergreen coniferous plantation, *Sci. China Ser. D Earth Sci.*, *52*, 257, doi:10.1007/s11430-009-0010-6.
Loya, W. M., L. C. Johnson, and K. J. Nadelhoffer (2004), Seasonal dynamics of leaf-and root-derived C in arctic tundra mesocosms, *Soil Biol. Biochem.*, *36*, 655–666, doi:10.1016/j.soilbio.2003.11.009.
Lucht, W., I. C. Prentice, R. B. Myneni, and S. Sitch (2002), Climatic control of the high-latitude vegetation greening trend and Pinatubo effect, *Science*, *296*, 1687–1689.
Lund, M., J. M. Falk, T. Friborg, H. N. Mbufong, C. Sigsgaard, H. Soegaard, and M. P. Tamstorf (2012), Trends in $CO_2$ exchange in a high Arctic tundra heath, 2000–2010, *J. Geophys. Res.*, *117*, G02001, doi:10.1029/2011JG001901.
Lüers, J., S. Westermann, K. Piel, and J. Boike (2014), Annual $CO_2$ budget and seasonal $CO_2$ exchange signals at a high Arctic permafrost site on Spitsbergen, Svalbard archipelago, *Biogeosciences*, *11*, 6307–6322, doi:10.1594/PANGAEA.809507.
Mackelprang, R., M. P. Waldrop, K. M. DeAngelis, M. M. David, K. L. Chavarria, S. J. Blazewicz, E. M. Rubin, and J. K. Jansson (2011), Metagenomic analysis of a permafrost microbial community reveals a rapid response to thaw, *Nature*, *480*(7377), 368–371, doi:10.1038/nature10576.
Mauritz, M., R. Bracho, G. Celis, J. Hutchings, S. M. Natali, E. Pegoraro, V. G. Salmon, C. Schädel, E. E. Webb, and E. A. G. Schuur (2017), Nonlinear $CO_2$ flux response to 7 years of experimentally induced permafrost thaw, *Global Change Biol.*, *11*(1), 034014), doi:10.1111/gcb.13661.
Mbufong, H. N., et al. (2014), Assessing the spatial variability in peak season $CO_2$ exchange characteristics across the Arctic tundra using a light response curve parameterization, *Biogeosciences*, *11*(17), 4897–4912, doi:10.5194/bg-11-4897-2014.
McGuire, A. D., et al. (2012), An assessment of the carbon balance of Arctic tundra: Comparisons among observations, process models, and atmospheric inversions, *Biogeosciences*, *9*(8), 3185–3204, doi:10.5194/bg-9-3185-2012.
McGuire, A. D., L. G. Anderson, T. R. Christensen, S. Dallimore, L. Guo, D. J. Hayes, M. Heimann, T. D. Lorenson, R. W. Macdonald, and N. Roulet (2009), Sensitivity of the carbon cycle in the Arctic to climate change, *Ecol. Monogr.*, *79*(4), 523–555.

Mohan, J. E., et al. (2014), Mycorrhizal fungi mediation of terrestrial ecosystem responses to global change: Mini-review, *Fungal Ecol.*, *10*, 3–19, doi:10.1016/j.funeco.2014.01.005.

Morgado, L. N., T. A. Semenova, J. M. Welker, M. D. Walker, E. Smets, and J. Geml (2016), Long-term increase in snow depth leads to compositional changes in arctic ectomycorrhizal fungal communities, *Global Change Biol.*, *22*, 3080–3096, doi:10.1111/gcb.13294.

Morgado, L. N., T. A. Semenova, J. M. Welker, M. D. Walker, E. Smets, and J. Geml (2015), Summer temperature increase has distinct effects on the ectomycorrhizal fungal communities of moist tussock and dry tundra in Arctic Alaska, *Global Change Biol.*, *21*(2), 959–972, doi:10.1111/gcb.12716.

Myers-Smith, I. H., B. C. Forbes, and M. Wilmking (2011), Shrub expansion in tundra ecosystems: Dynamics, impacts and research priorities, *Environ. Res. Lett.*, *6*, 15, doi:10.1088/1748-9326/6/4/045509.

Myklebust, M. C., L. E. Hipps, and R. J. Ryel (2008), Comparison of eddy covariance, chamber, and gradient methods of measuring soil $CO_2$ efflux in an annual semi-arid grass, *Bromus tectorum*, *Agric. For. Meteorol.*, *148*(11), 1894–1907, doi:10.1016/j.agrformet.2008.06.016.

Natali, S. M., et al. (2015), Permafrost thaw and soil moisture driving $CO_2$ and $CH_4$ release from upland tundra, *J. Geophys. Res. Biogeosci.*, *120*, 525–537, doi:10.1002/2014JG002872.

Natali, S. M., E. A. G. Schuur, and C. Trucco (2011), Effects of experimental warming of air, soil and permafrost on carbon balance in Alaskan tundra, *Global Change Biol.*, *17*, 1394–1407, doi:10.1111/j.1365-2486.2010.02303.x.

Natali, S. M., E. A. G. Schuur, and R. L. Rubin (2012), Increased plant productivity in Alaskan tundra as a result of experimental warming of soil and permafrost, *J. Ecol.*, *100*(2), 488–498, doi:10.1111/j.1365-2745.2011.01925.x.

Natali, S. M., E. A. G. Schuur, E. E. Webb, C. E. H. Pries, and K. G. Crummer (2014), Permafrost degradation stimulates carbon loss from experimentally warmed tundra, *Ecology*, *95*(3), 602–608, doi:10.1890/13-0602.1.

Nowinski, N. S., L. Taneva, S. E. Trumbore, and J. M. Welker (2010), Decomposition of old organic matter as a result of deeper active layers in a snow depth manipulation experiment, *Oecologia*, *163*(3), 785–792, doi:10.1007/s00442-009-1556-x.

Oberbauer, S. F., et al. (2013), Phenological response of tundra plants to background climate variation tested using the International Tundra Experiment, *Philos. Trans. R. Soc., B*, *368*(1624), 1–13, doi:10.1098/rstb.2012.0481.

Oberbauer, S. F., C. E. Tweedie, and J. M. Welker (2007), Tundra $CO_2$ fluxes in response to experimental warming across latitudinal and moisture gradients, *Ecol. Monogr.*, *77*, 221–238.

Oechel, W. C., C. A. Laskowski, and G. Burba (2014), Annual patterns and budget of $CO_2$ flux in an Arctic tussock tundra ecosystem, *J. Geophys. Res. Biogeosci.*, *119*, 323–339, doi:10.1002/2013JG002431.

Oechel, W. C., G. L. Vourlitis, S. Brooks, T. L. Crawford, and E. Dumas (1998), Intercomparison among chamber, tower, and aircraft net $CO_2$ and energy fluxes measured during the Arctic System Science Land-Atmosphere-Ice Interactions (ARCSS-LAII) Flux Study, *J. Geophys. Res.*, *103*(D22), 28,993–29,003, doi:10.1029/1998JD200015.

Oechel, W. C., G. Vourlitis, and S. J. Hastings (1997), Cold season $CO_2$ emission from arctic soils, *Global Biogeochem. Cycles*, *11*(2), 163–172.

Olsrud, M., and T. R. Christensen (2004), Carbon cycling in subarctic tundra; seasonal variation in ecosystem partitioning based on in situ $^{14}C$ pulse-labelling, *Soil Biol. Biochem.*, *36*(2), 245–253, doi:10.1016/j.soilbio.2003.08.026.

Osterkamp, T. E., and V. E. Romanovsky (1999), Evidence for warming and thawing of discontinuous permafrost in Alaska, *Permafrost Periglacial Process*, *10*, 17–37, doi:10.1002/(SICI)1099-1530(199901/03)10:1<17::AID-PPP303>3.0.CO;2-4.

Parker, T. C., J.-A. Subke, and P. A. Wookey (2015), Rapid carbon turnover beneath shrub and tree vegetation is associated with low soil carbon stocks at a subarctic treeline, *Global Change Biol.*, *21*(5), 2070–2081, doi:10.1111/gcb.12793.

Pearson, R. G., S. J. Phillips, M. M. Loranty, P. S. A. Beck, T. Damoulas, S. J. Knight, and S. J. Goetz (2013), Shifts in Arctic vegetation and associated feedbacks under climate change, *Nat. Clim. Change*, *3*(4), 1–5, doi:10.1038/nclimate1858.

R Development Core Team (2015), *R: A Language and Environment for Statistical Computing*, R Foundation for Statistical Computing, Vienna.

Riederer, M., A. Serafimovich, and T. Foken (2014), Net ecosystem $CO_2$ exchange measurements by the closed chamber method and the eddy covariance technique and their dependence on atmospheric conditions, *Atmos. Meas. Tech.*, *7*(4), 1057–1064, doi:10.5194/amt-7-1057-2014.

Romanovsky, V. E., S. L. Smith, H. H. Christiansen, N. I. Shiklomanov, D. S. Drozdov, N. G. Oberman, A. L. Kholodov, and S. S. Marchenko (2011), Permafrost, in Arctic Report Card 2011.

Rustad, L. E., T. G. Huntington, and R. D. Boone (2000), Controls on soil respiration: Implications for climate change, *Biogeochemistry*, *48*, 1–6.

Salmon, V. G., P. Soucy, M. Mauritz, G. Celis, S. M. Natali, M. C. Mack, and E. A. G. Schuur (2016), Nitrogen availability increases in a tundra ecosystem during five years of experimental permafrost thaw, *Global Change Biol.*, *22*(5), 1927–1941, doi:10.1111/gcb.13204.

Schädel, C., E. A. G. Schuur, R. Bracho, B. Elberling, C. Knoblauch, H. Lee, Y. Luo, G. R. Shaver, and M. R. Turetsky (2014), Circumpolar assessment of permafrost C quality and its vulnerability over time using long-term incubation data, *Global Change Biol.*, *20*(2), 641–652, doi:10.1111/gcb.12417.

Schimel, D. S. (1995), Terrestrial ecosystems and the carbon cycle, *Global Change Biol.*, *1*(1), 77–91, doi:10.1111/j.1365-2486.1995.tb00008.x.

Schimel, J. P., J. Fahnestock, G. Michaelson, C. Mikan, C. L. Ping, V. E. Romanovsky, and J. Welker (2006), Cold-season production of $CO_2$ in arctic soils: Can laboratory and field estimates be reconciled through a simple modeling approach?, *Arct. Antarct. Alp. Res.*, *38*(2), 249–256, doi:10.1657/1938-4246-44.4.446.

Schuur, E. A. G., K. G. Crummer, J. G. Vogel, and M. C. Mack (2007), Plant species composition and productivity following permafrost thaw and thermokarst in Alaskan tundra, *Ecosystems*, *10*(2), 280–292, doi:10.1007/s10021-007-9024-0.

Schuur, E. A. G., J. G. Vogel, K. G. Crummer, H. Lee, J. O. Sickman, and T. E. Osterkamp (2009), The effect of permafrost thaw on old carbon release and net carbon exchange from tundra, *Nature*, *459*(7246), 556–559, doi:10.1038/nature08031.

Schuur, E. A. G., et al. (2015), Climate change and the permafrost carbon feedback, *Nature*, *520*(7546), 171–179, doi:10.1038/nature14338.

Semenova, T. A., L. N. Morgado, and J. M. Welker (2015), Long-term experimental warming alters community composition of ascomycetes in Alaskan moist and dry arctic tundra, *Mol. Ecol.*, *24*, 424–437, doi:10.1111/mec.13045.

Sharp, E. D., P. F. Sullivan, H. Steltzer, A. Z. Csank, and J. M. Welker (2013), Complex carbon cycle responses to multi-level warming and supplemental summer rain in the high Arctic, *Global Change Biol.*, *19*(6), 1780–1792, doi:10.1111/gcb.12149.

Shaver, G. R., and J. Kummerow (1992), Phenology, resource allocation, and growth of arctic vascular plants, in *Arctic Ecosystems in a Changing Climate: An Ecophysiological Perspective*, edited by F. S. Chapin et al., pp. 193–211, Academic Press, San Diego, Calif.

Shaver, G. R., and W. D. Billings (1975), Root production and root turnover in a wet tundra ecosystem, barrow, Alaska, *Ecology*, *56*(2), 401–409.

Shaver, G. R., F. Chapin III, and B. L. Gartner (1986), Factors limiting seasonal growth and peak biomass accumulation in *Eriophorum vaginatum* in Alaskan tussock tundra, *J. Ecol.*, *74*(1), 257–278.

Smith, W. K., R. D. Kelly, J. M. Welker, J. T. Fahnestock, W. A. Reiners, and R. Hunt (2003), Leaf-to-aircraft measurements of net $CO_2$ exchange in a sagebrush steppe ecosystem, *J. Geophys. Res.*, *108*(D3), 4122, doi:10.1029/2002JD002512.

Sturm, M., T. Douglas, C. Racine, and G. E. Liston (2005), Changing snow and shrub conditions affect albedo with global implications, *J. Geophys. Res.*, *110*, G01004, doi:10.1029/2005JG000013.

Sullivan, P. F., and J. M. Welker (2005), Warming chambers stimulate early season growth of an arctic sedge: Results of a minirhizotron field study, *Oecologia*, *142*(4), 616–626, doi:10.1007/s00442-004-1764-3.

Sullivan, P. F., J. M. Welker, S. J. T. Arens, and B. Sveinbjörnsson (2008), Continuous estimates of $CO_2$ efflux from arctic and boreal soils during the snow-covered season in Alaska, *J. Geophys. Res.*, *113*, G04009, doi:10.1029/2008JG000715.

Sullivan, P. F., M. Sommerkorn, H. M. Rueth, K. J. Nadelhoffer, G. R. Shaver, and J. M. Welker (2007), Climate and species affect fine root production with long-term fertilization in acidic tussock tundra near Toolik Lake, Alaska, *Oecologia*, *153*(3), 643–652, doi:10.1007/s00442-007-0753-8.

Tarnocai, C., J. G. Canadell, E. A. G. Schuur, P. Kuhry, G. Mazhitova, and S. Zimov (2009), Soil organic carbon pools in the northern circumpolar permafrost region, *Global Biogeochem. Cycles*, *23*, GB2023, doi:10.1029/2008GB003327.

Thornley, J. H. M., and I. R. Johnson (1990), *Plant and Crop Modelling: A Mathematical Approach to Plant and Crop Physiology*, pp. 1–669, Clarendon Press, Oxford, U. K.

Trucco, C., E. A. G. Schuur, S. M. Natali, E. F. Belshe, R. Bracho, and J. Vogel (2012), Seven-year trends of $CO_2$ exchange in a tundra ecosystem affected by long-term permafrost thaw, *J. Geophys. Res.*, *117*, G02031, doi:10.1029/2011JG001907.

Vogel, J., E. A. G. Schuur, C. Trucco, and H. Lee (2009), Response of $CO_2$ exchange in a tussock tundra ecosystem to permafrost thaw and thermokarst development, *J. Geophys. Res.*, *114*, G04018, doi:10.1029/2008JG000901.

Walker, D. A., et al. (2012), Environment, vegetation and greenness (NDVI) along the North America and Eurasia Arctic transects, *Environ. Res. Lett.*, *7*(1), 015504), doi:10.1088/1748-9326/7/1/015504.

Walker, M. D., et al. (2006), Plant community responses to experimental warming across the tundra biome, *Proc. Natl. Acad. Sci. U.S.A.*, *103*(5), 1342–1346, doi:10.1073/pnas.0503198103.

Wang, W. J., Y. G. Zu, H. M. Wang, T. Hirano, and K. Takagi (2005), Effect of collar insertion on soil respiration in a larch forest measured with a LI-6400 soil $CO_2$ flux system, *J. For. Res.*, *15*, 901–913, doi:10.1111/j.1365-2486.2008.01757.x.

Webb, E. E., et al. (2016), Increased wintertime $CO_2$ loss as a result of sustained tundra warming, *J. Geophys. Res. Biogeosci.*, *121*, 249–265, doi:10.1002/2014JG002795.

Webb, E. K., G. I. Pearman, and R. Leuning (1980), Correction of flux measurements for density effects due to heat and water-vapor transfer, *Q. J. R. Meteorol. Soc.*, *106*(447), 85–100.

Welker, J. M., J. T. Fahnestock, and K. L. Povirk (2004), Alpine grassland $CO_2$ exchange and nitrogen cycling: Grazing history effects, medicine bow range, Wyoming, USA, *Arctic*, *36*, 11–20, doi:10.1657/1523-0430(2004)036%5B0011:AGCEAN%5D2.0.CO;2.

Welker, J. M., J. T. Fahnestock, and M. H. Jones (2000), Annual $CO_2$ flux in dry and moist arctic tundra: Field responses to increases in summer temperatures and winter snow depth, *Clim. Change*, *44*(1–2), 139–150.

Xue, K., et al. (2016), Tundra soil carbon is vulnerable to rapid microbial decomposition under climate warming, *Nat. Clim. Change*, *6*, 595–600, doi:10.1038/nclimate2940.

Zamolodchikov, D. G., D. V. Karelin, A. I. Ivaschenk, W. C. Oechel, and S. J. Hastings (2003), $CO_2$ flux measurements in Russian Far East tundra using eddy covariance and closed chamber techniques, *Tellus B Chem. Phys. Meteorol.*, *55*(4), 879–892.

Zona, D., D. A. Lipson, J. H. Richards, G. K. Phoenix, A. K. Liljedahl, M. Ueyama, C. S. Sturtevant, and W. C. Oechel (2014), Delayed responses of an Arctic ecosystem to an extreme summer: Impacts on net ecosystem exchange and vegetation functioning, *Biogeosciences*, *11*(20), 5877–5888, doi:10.5194/bg-11-5877-2014-supplement.